Electric Power Systems Research 132 (2016) 9–21

Contents lists available at ScienceDirect

Electric Power Systems Research

journal homepage: www.elsevier.com/locate/epsr

Out-of-step protection of generator using analysis of angular velocity and acceleration data measured from magnetic flux

Hamid Yaghobi*

Faculty of Electrical and Computer Engineering, Semnan University, Semnan, Iran

ARTICLE INFO

Article history:
Received 8 August 2015
Received in revised form 14 October 2015
Accepted 5 November 2015

Keywords:
Synchronous generator
Out-of-step protection
Magnetic flux

ABSTRACT

This paper presents a new flux-based method for out-of-step protection of synchronous generator. The available measured angular velocity and acceleration data from magnetic flux of the generator, at the location of the relay, are used to detect out-of-step conditions. An out-of-step condition can be distinguished in the point in which the polarity of the angular acceleration changes from a negative to positive value and the angular velocity is greater than the base angular velocity. The basic idea of the approach stems from the fact that the resultant magnetic flux rotates at synchronous speed and cannot change rapidly. In other words, this constant magnetic flux will not be affected by switching transients due to highly inductive characteristics of the machine. Finally, the simulation results verify the straightforward application of the proposed technique even for a multi-machine power system. Therefore, the proposed approach can be directly applied to an interconnected power system without any need to cumbersome network reduction methods. Furthermore, the proposed technique does not require any offline studies and overcomes some of the problems associated with the previous solutions.

1. Introduction

The North American blackout on August 14, 2003, has led to considerable number of researches on many aspects of system protection. One of the important and commonly misunderstood issues that have been addressed is power swing and out-of-step protection applied to the power systems [1]. The power system stability problem is a major concern in the planning and operation of electric power systems, and synchronous generators play a significant role in this issue. An unstable power system that loses synchronism may cause severe damage to the machine, interruption of electrical supply, and significant economic loss. Therefore, loss of synchronism detection is essential for the safe operation of the system. Loss of synchronism of a synchronous generator may occur as a result of loss of excitation or out-of-step conditions. In loss of excitation fault, the excitation system may be completely or partially lost due to some technical problems [2]. However, in out-of-step conditions; the protection system also detects loss of synchronism, but with the excitation system intact. In out-of-step condition, the power system loses synchronism due to a disturbance such as short-circuit faults, line switching, generator tripping, load shedding, etc. [3,4]. Depending on the disturbance severity, the power network may or may not return to a new stable situation. When the disturbance is serious, the fluctuations would not be damped out which leads to asynchronous operation of the generators. This phenomenon is called out-of-step condition [4,5].

The most popular and commonly used approaches for detecting out-of-step conditions are based on the measurement of positive sequence impedance at the relay location. In general, these approaches utilize a distance relay with blinders in the R–X plane and a timer. Regardless of stable or unstable swing, the distance relay is prone to interpret a power swing as a fault which is discussed in Fig. 1. The relay in Fig. 1(a) trips for the cases 'b' and 'c' as the impedance trajectory moves towards the operating zone. Sending a trip signal during the stable condition (case 'b') is not desirable. Therefore, assigning a time delay is usually utilized to overcome the possible maloperation of the distance relay. In this case, the power network returns to the new steady state condition. Thus, an out-of-step protection relay must be able to discriminate between a fault and a swing (stable or unstable). First, the blocking function must block relay during a stable or unstable power swing. Tripping function must then distinguish between stable and unstable power swings.

It must be mentioned that according to the power system configuration, loading conditions, the type of faults that often happen on the system and the desired performance, one of the blinder schemes, can be selected. The schemes can be classified as one blinder scheme, two blinder scheme, concentric characteristic schemes

* Tel.: +: +98 9116419238.
E-mail address: yaghobi@semnan.ac.ir

http://dx.doi.org/10.1016/j.epsr.2015.11.003
0378-7796/

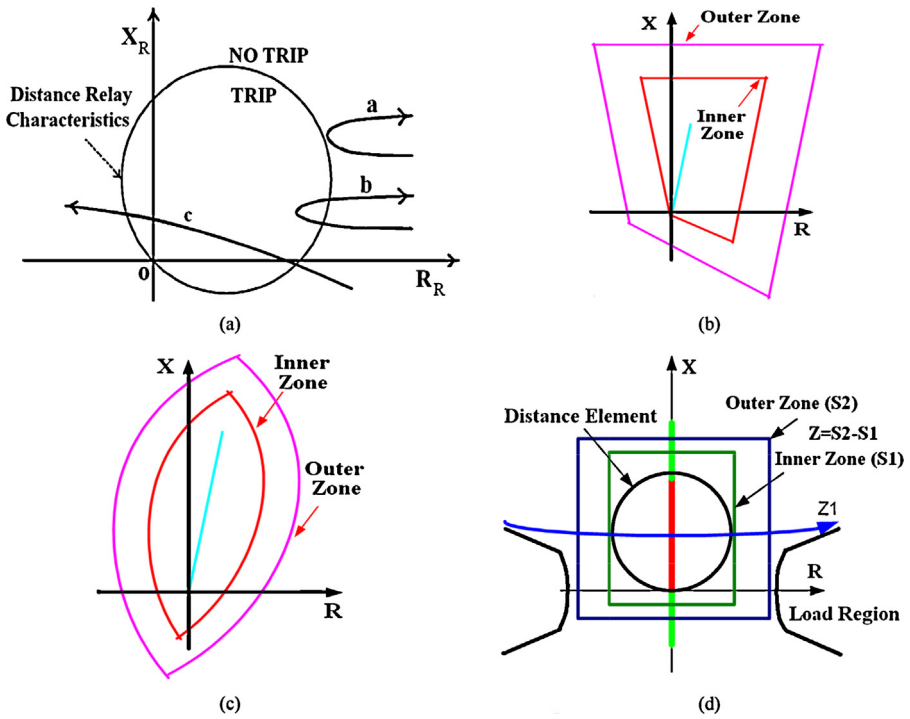

Fig. 1. Impedance-based techniques of out-of-step protection relay [1]: (a) operating characteristics of distance relay showing various power swings; (b) concentric quadrilaterals; (c) concentric lenticulars; (d) concentric rectangular.

(Mho, Polygon, Lenticular). Fig. 1(b)–(d) illustrate the concentric characteristic schemes used for out-of-step protection and it must be noted that the operating principle is the same for all cases.

During normal conditions, the impedance measured at the relay location is the load impedance, and its trajectory is away from the distance characteristics. During a fault occurrence, the impedance trajectory seen from the terminal of the generator travels immediately from the load impedance region to the location that shows the fault on the R–X plane. During a power swing condition, the calculated impedance moves slowly on the R–X plane due to the slip frequency of an equivalent two-machine system. Traditional detection methods for power swing condition, utilize the difference between the impedance rate of change in a fault and in a power swing condition to discriminate between a fault and a swing. In order to carry out this discrimination, one specific designer can usually place two concentric impedance characteristics '*S*1' and '*S*2', separated by impedance *Z* (*Z* = *S*2 − *S*1), on the R–X plane (see Fig. 1(d)). The time taken by the impedance locus to travel between the two concentric impedances ('*S*1' and '*S*2') is measured by the relay. This time is compared with the preset time to distinguish between a fault and a swing. If the impedance locus travels inner and outer characteristics in less than the pre-set time, the relay detects the case to be a fault. If the impedance locus passes the outer characteristic, but does not pass the inner characteristic, the case is a stable swing. Finally, an out-of-step condition is detected when the time it takes for the impedance locus to pass through both inner and outer characteristics is more than the pre-set time [1,4].

Setting the blinders (i.e. the inner characteristics '*S*1' and the outer characteristics '*S*2') and determining a pre-set delay are the main problems with these methods. The settings require some information about the rate of slip during the transient condition that depends on the accelerating torque and power network inertias. Another problem is that in heavily loaded long transmission line condition, the load region lies close to the operating characteristics of the relay and the settings of binders may overlap the setting of relay and normal load region. This overlap may cause the relay incorrect operation.

It can be clearly seen that, these methods need some information about the normal operation region, the system loading conditions, the possible swing frequencies, the fastest power swing and other system specific data. In other words, these methods need an extensive system stability studies for finding the settings and their complexity increases when applied to multi-machine networks. For a multi-machine network, the realization of these methods is not clear-cut and is not straightforward as a two area system. It is worth mentioning that, incorrect operation of these relays has been reported in recent works [1,6], when there is a significant change in system and transfer impedance values. Therefore, in order to enhance security and also overcome some of the problems associated with the impedance-based techniques, new methods have been introduced in literature.

In [1], the monitoring of the rate of change of swing center voltage (SCV) was found to be an effective technique to discriminate between stable and out-of-step swings. The disadvantage of this method is that for a multi-machine network, the voltage measured at relay location does not give a precise estimation of SCV. The method also needs extensive offline system stability simulations to set the rate of change of SCV (threshold value) [4]. Out-of-step detection method by mapping the equal area criterion conditions to the time domain is presented in [4]. Out-of-step conditions were identified using the accelerating and decelerating energies, which represents the area under the power-time curve. The recommended technique is simple and overcomes some of the problems associated with the previous methods. However, this identification is graphically done by point-by-point analysis directly in the time domain that may limit its application. A new out-of-step detection method using the state-plane representation of the generator speed and power angle is presented [6]. The energy function criterion for out-of-step detection in a complex power system has been proposed in [7]. However, due to its dependency to wide area information, its implementation becomes complex [4].

Some references by using different approaches, such as fuzzy inference and artificial neural networks (ANNs) have been tried to improve out-of-step protection [7,8]. However, the methods require a large amount of training data to train for all probable swing scenarios which makes it complicated and time-consuming.

It worths noting that measuring of the generator's angular velocity and acceleration data from different inputs have been presented in literature [3,9]. In [9], angular velocity data measured directly from the rotors have been used in out-of-step prediction. In this technique, angular velocity data are measured by sensors and gears which are fastened directly to the rotors. Out-of-step condition between two groups of generators can be then predicted. However, a special configuration of the equipments, wide area information and synchronization of measurements are required in this method. Furthermore, torsional oscillation of the rotor is a problem of this technique. In fact, in nuclear and thermal power plants, turbine and generator masses are connected to the same rotor. In this configuration, when a disturbance happens, the mass of the rotor will be distorted between the two masses and the angular velocity measurement will be affected by this torsional oscillation. In addition, reference [3] proposed a new algorithm for detecting out-of-step conditions based on phasor angular velocity and acceleration of the terminal voltage of the machine at the local bus. However, the terminal voltage of the machine will be affected by the switching transients in the power networks.

On the other hand, fault monitoring of electrical machines using magnetic flux measurements have been proposed as a typical subject of investigation in recent works [10,11]. It has been proven that the condition monitoring of electrical machines based on magnetic flux criterion is an efficient technique for fault detection. Furthermore, this criterion has been used successfully for diagnosis of the internal faults [12–14] and loss of excitation protection [15–17] in synchronous generators by the author.

In a continuation of the previous works, this paper presents a new out-of-step prediction algorithm using the measured angular velocity and acceleration data from magnetic flux of the generator that are available at the location of the relay. The proposed method has been tested on a single-machine infinite bus (SMIB), a three-machine infinite bus (TMIB) and an IEEE 30-bus power system using Matlab/Simulink software. Some comparisons are made with some existing methods by considering different generator sizes. The simulation results show that the proposed method discriminated between stable and unstable conditions, satisfactorily. The new relay is independent from other generator conventional protections without any coordination studies. Moreover, it is not affected by the machine size, power system configuration and its parameters.

2. Magnetic flux as the main criterion for out-of-step protection

This section explores why magnetic flux is selected as the main criterion for out-of-step detection.

2.1. Main criterion

In a salient-pole synchronous generator that is shown in Fig. 2(a), as the rotor turns, the magnetic flux changes cosinusoidally with the angle between the magnetic axes of the rotor and stator coil. With the rotor spinning at constant angular velocity w_m, the magnetic flux in phase a of the stator coil can be found as follows [18]:

$$\lambda_a = N_{ph}\phi_P \cos\left(\frac{\text{poles}}{2} w_m t\right) = N_{ph}\phi_P \cos(w_e t), \quad w_e = \left(\frac{\text{poles}}{2}\right) w_m \tag{1}$$

where N_{ph} is total series turns in the stator winding and ϕ_P is the air-gap flux per pole (see Fig. 2(a)). By Faraday's law, the voltage induced in phase a can be calculated as follows:

$$E_a = \frac{-d\lambda_a}{dt} = -N_{ph}\frac{d\phi_P}{dt} \cos w_e t + w_e N_{ph}\phi_P \sin(w_e t) \tag{2}$$

The first term on the right-hand side of (2) is a transformer voltage and is presented only when the amplitude of the magnetic air-gap flux wave varies with time. The second term is the speed voltage produced by the relative motion of the magnetic air-gap flux wave on the stator winding. It must be noted, in the normal steady-state condition, the amplitude of the magnetic air-gap flux wave is constant; under these situations the first term is zero and the produced voltage is only the speed voltage. Therefore, with constant magnetic air-gap flux, the induced voltage in phase a can be calculated as follows:

$$E_a = w_e N_{ph}\phi_P \sin(w_e t) \tag{3}$$

Although this induced voltage is obtained on the assumption that only the excitation winding is generating air-gap flux, the equation applies equally well to the general condition where ϕ_P is the net magnetic air-gap flux per pole generated by currents on both the rotor and the stator windings.

The effect of the winding distribution factor should be considered in this induced voltage. If there are n slots per phase, each with voltage E_{ai}, where the phase angle of each voltage increases by γ° from slot to slot (see Fig. 2(b)), the resulting voltage E_a can be found as follows:

$$E_a = E_{a1} + E_{a2} + \ldots + E_{an} \tag{4}$$

In addition, the effect of the fractional pitch coil also must be considered. The combination of these two effects can be included in a winding factor k_w to be used as a reduction factor in (3). Thus, the induced voltage per phase can be calculated as follows:

$$E_a = w_e k_w N_{ph}\phi_p \sin(w_e t) \tag{5}$$

On the other hand, winding configurations of the machine also affects the resulting voltage E_a. For example, schematic view of a two-pole generator with two possible winding configurations is shown in Fig. 2(c). In this figure, a two parallel circuits winding and a two series connected circuits per phase is illustrated. Finally, as stated earlier, switching transients in the power system affects the terminal voltage of the machine which can change very quickly [6]; while due to highly inductive characteristics of the machine, the magnetic flux is not affected by switching transients. According to the above discussions, it can be clearly seen that, the resulting voltage E_a is affected by the winding factor, winding configurations and switching transients; while the air-gap flux per pole (ϕ_P) is independent from these causes and is constant. It must be noted, magnetic flux is a local variable in the machine and this criterion will change locally due to the fault occurrence, whereas stator current and voltage are global external variables that are affected by different causes. Therefore, air-gap flux per pole is a suitable criterion for fault detection in electrical machines.

2.2. Magnetic flux measurement

Search coil sensors wounded about stator teeth, are widely used within the electrical machines [14,20] to provide high-accuracy

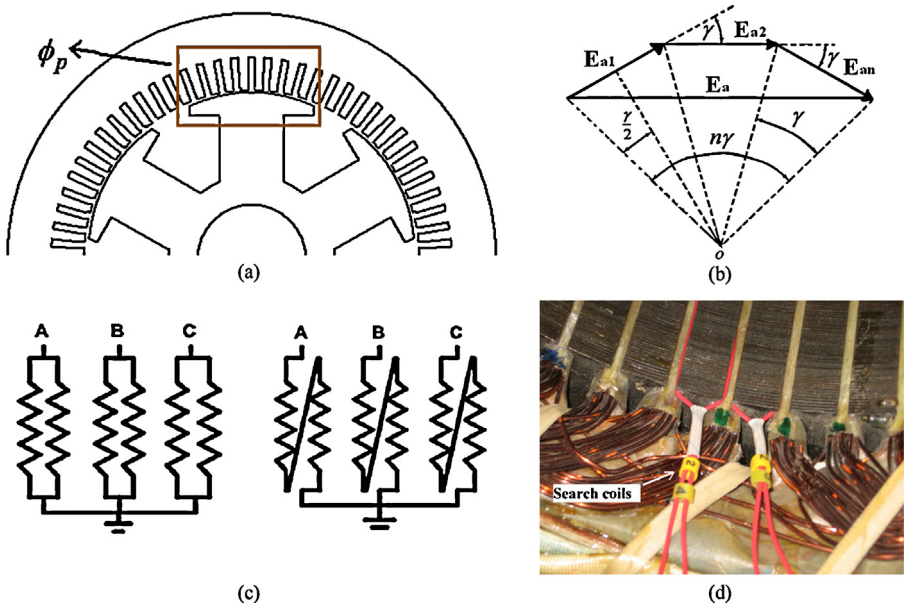

Fig. 2. Synchronous generator: (a) cross-sectional view; (b) coil voltage phasors [18]; (c) a two parallel and series connected circuits per phase [19]; (d) search coil sensors for high-accuracy measurement of the magnetic flux

measurement of the machine magnetic flux as shown in Fig. 2(d). A search coil is able to detect magnetic fields as weak as 2×10^{-5} nT, and no upper limit has been specified for its sensitivity range. These sensors have robust characteristics such as insensitivity to external situations (temperature and humidity), in very hostile environments. Search coil sensors should be placed in the stator slots of the machine that this work is easy for the manufacturer or should be placed in the stator slots by the user at overhaul time of the machine. The major disadvantage of these sensors is that they are invasive. However, due to possible damages that can be introduced to the machine, the installation of these sensors is usually avoided. There seems to be clear and realistic that if the suitable search coils are used, the damages can be made negligible. The search coil sensors are now becoming common on synchronous generators. It is worth highlighting that, these sensors have been used for flux measurement in a large number of synchronous generators in the Central Electricity Generating Board [20]. As stated earlier, air-gap flux per pole (ϕ_P) is required for the proposed technique in this paper that can be achieved from the summation of the fluxes over the related search coils as shown in Fig. 2(a) and (d).

In order to show the concept of the magnetic flux measurement, a test bed has been implemented on a real 50 kVA, 3-phase synchronous generator. Search coil sensors and designed data acquisition card are used for measuring the stator magnetic flux. Serial port interface has been utilized for connecting the data acquisition card to the computer and these data are communicated to the computer. These data can be processed and analyzed. More details about this measuring system are explained in [13,14,17].

2.3. Proposed algorithm

It is clear that, if three balanced currents flow in a balanced three-phase winding, a magnetic flux of constant magnitude is produced in the air-gap of the machine. The magnetic flux produced by the stator is designated as ϕ_S and the magnetic flux produced by the rotor is designated as ϕ_F (see Fig. 3(a)). The resultant constant magnetic flux is: $\phi_R = \phi_S + \phi_F$ that rotates at synchronous speed. Phasor diagrams for a typical synchronous machine under generator operation conditions are presented in Fig. 3(b) and (c). According to these figures, it can be seen that, under normal conditions with different operating modes, a magnetic flux by constant magnitude is produced in the air-gap of the machine and rotates around the machine at a frequency equal to the frequency of the currents flowing through the winding. Fig. 3(b) and (c) show how the stator-produced flux affects the rotor-produced flux for leading and lagging power factors. This phenomenon is called armature reaction effect. It must be noted that the synchronous speed of the rotating flux is not affected by the magnetizing and demagnetizing effects (armature reaction). However, the out-of-step condition of the generator affects the synchronous speed of the rotating magnetic flux and changes it. This change will be reflected in the argument of the rotating magnetic flux. In addition, the phasor diagrams from different data windows of the $\phi_R(t)$ is illustrated in Fig. 3(d) which revolves in a counterclockwise direction in the complex plane.

In the proposed method, the angular velocity and acceleration data measured from magnetic flux of the generator are used to detect out-of-step condition. First, the average of the angular velocity has been calculated over a $2N+1$ data window as follows:

$$w_{avg}(k) = \sum_{k=-N}^{N} \frac{\angle\phi(k) - \angle\phi(k-1)}{T} \tag{6}$$

where k is the sample number and T is the sampling interval. Second, the average of the angular acceleration has been calculated as follows:

$$\alpha_{avg}(k) = \sum_{k=-N}^{N} \frac{\angle w(k) - \angle w(k-1)}{T} \tag{7}$$

On the other hand, the measured angular and acceleration velocity from the phasor of the terminal voltage are proportional to the measured ones from the generator angle [3]. Therefore, due to the relationships between the voltage and magnetic flux, Eqs. (8)–(10) can be derived as follows:

$$w_\phi \cong w_0 + \frac{w_d(t)}{2}, \quad w_d(t) = \frac{d\delta(t)}{dt} \tag{8}$$

$$\alpha_\phi \cong \frac{\alpha_d(t)}{2}, \quad \alpha_d(t) = \frac{d^2\delta(t)}{dt^2} \tag{9}$$

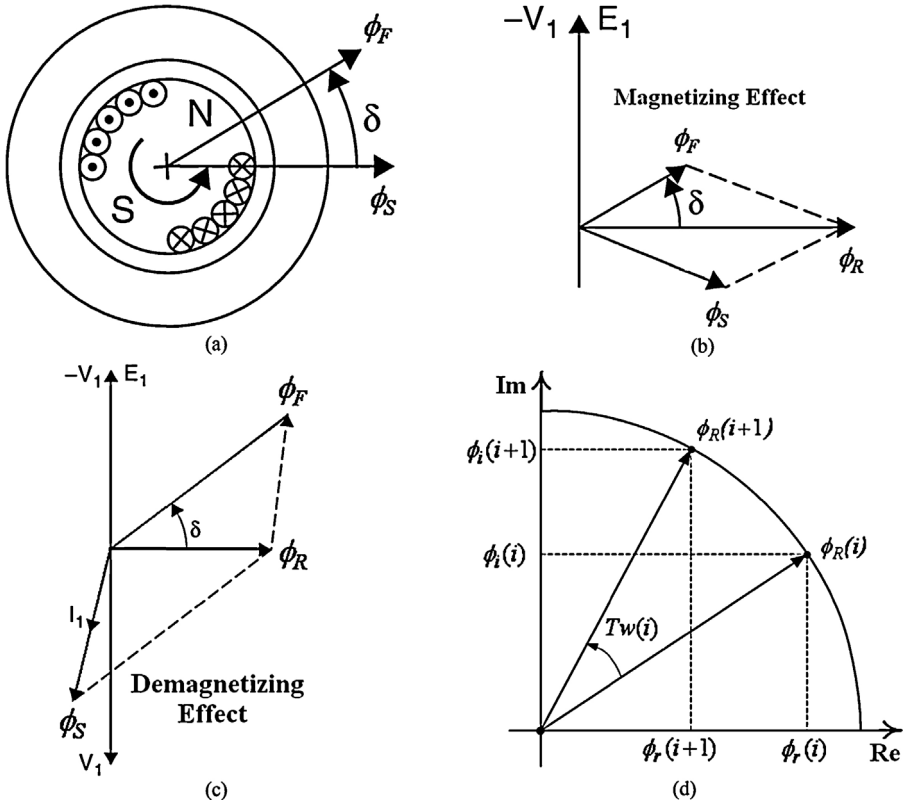

Fig. 3. Phasor diagrams for a synchronous generator [19]: (a) magnetic fields produced by the stator and rotor; (b) PF Leading; (c) PF lagging; (d) phasor diagram for $\phi_R(t)$.

$$w_\phi \cong w_0 + \frac{d\delta(t)/dt}{2}, \quad \alpha_\phi \cong \frac{d^2\delta(t)/dt^2}{2} \tag{10}$$

where $w_d(t)$ and $\alpha_d(t)$ are the angular velocity and acceleration of the angle δ, respectively. The angle δ is known as the generator angle. Furthermore, the equation that describes the dynamic behavior of the machine is the swing equation as follows:

$$\frac{M}{w_s}\frac{d^2\delta}{dt^2} = p_m - p_e = p_A \tag{11}$$

where M is the machine inertia constant, p_e is the electrical power, p_m is the mechanical power, p_A is the accelerating power and w_s is the frequency of the system.

Fig. 4(a) and (b) show the power angle curve in case of a stable and an unstable swing, respectively. The two curves are utilized to show the classical equal area criterion (EAC) in the δ domain. The trajectory of the angular velocity and acceleration data measured from the magnetic flux corresponding to the stable and the unstable swing conditions are shown in Fig. 4(c) and (d), respectively. These curves are utilized to explain the proposed method. Based on equations (8)-(11), the details of the relationships between the position of the operating point on the p–δ curve and the w_ϕ–α_ϕ plane are shown in Tables 1 and 2.

In these tables, it can be clearly seen that the out-of-step condition can be detected by utilizing the angular velocity and acceleration data that are measured from the magnetic flux. In this method, the generator will go out-of-step condition when the polarity of the average of angular acceleration changes from a negative to positive value and the average of angular velocity is greater than the base angular velocity ($w_0 = 377$ rad/s); otherwise, it will remain stable i.e. the following conditions must be satisfied for the out-of-step condition.

$$\begin{aligned} &\alpha_\phi(k-1) < 0 \quad \text{and} \quad \alpha_\phi(k) > 0\& \\ &w_\phi(k) > w_0 \Rightarrow \text{Out-of-step condition} \end{aligned} \tag{12}$$

Fig. 5(a) illustrates a typical behavior of the angular velocity and acceleration data measured from the magnetic flux of the generator available at the location of the relay following out-of-step condition.

For creating the out-of-step condition, a three-phase fault is applied three seconds after the start of the simulation time for the duration of 0.3 s. According to this figure, it can be clearly seen that for this unstable power swing, the out-of-step detection by the proposed method is satisfied 0.451 s (3.451 − 3) after the inception of the three-phase fault. The algorithm of the proposed method is summarized in the flowchart shown in Fig. 5(b).

2.4. Saturation effect

In the following, the effect of saturation phenomenon on the performance of the proposed relay is investigated in two subsections.

2.4.1. Saturation due to exciter operation

Power system generators employ automatic voltage regulators (AVRs) in their control systems. AVR controls the output voltage and the magnetic flux of the generator by controlling its excitation current. In other words, AVR maintaining the level of the excitation field V_{fd} in the rotor windings at the value needed to keep the stator voltage near to the desired set-point. Moreover, saturation limits are used in the AVR to account for the maximum permissible current in the exciter, i.e. V_{fd} has an upper limit value $V_{f\max}$ and a lower limit value $V_{f\min}$ (see Fig. 7(c)). Consequently, AVR and

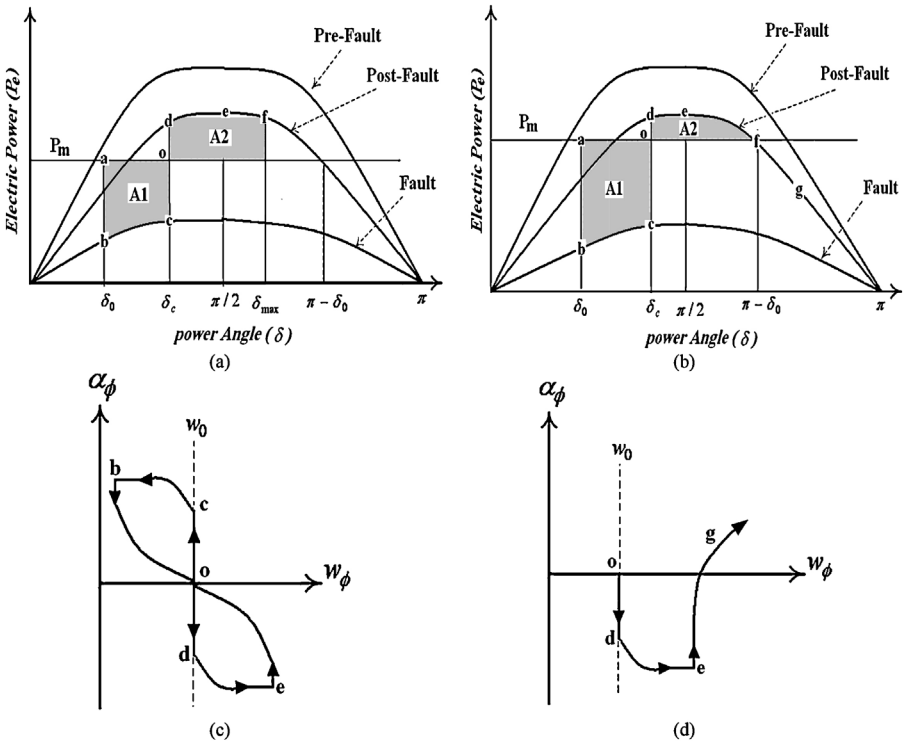

Fig. 4. Stable and unstable swing conditions: (a) power–angle curve in case of a stable swing; (b) power–angle curve in case of an unstable swing; (c) angular velocity and acceleration of $\phi(t)$ in case of a stable swing; (d) the angular velocity and acceleration of $\phi(t)$ in case of an unstable swing.

Table 1
The details of the relationships between the position of the operating point on the p–δ curve and the w_ϕ–α_ϕ plane in the case of stable swing.

Operating point	The generator angle swings in o-d-e-f-o-c-b-o points	
	Angular velocity and acceleration of δ	Angular velocity and acceleration of $\phi(t)$
O	$p_e = p_m,\ p_A = 0,\ \frac{d\delta(t)}{dt} = 0,\ \frac{d^2\delta(t)}{dt^2} = 0$	$w_\phi = w_0,\ \alpha_\phi = 0$
D	$p_e > p_m,\ p_A < 0,\ \frac{d\delta(t)}{dt} = 0,\ \frac{d^2\delta(t)}{dt^2} < 0$	$w_\phi = w_0,\ \alpha_\phi < 0$
E	$p_e > p_m,\ p_A < 0,\ \frac{d\delta(t)}{dt} > 0,\ \frac{d^2\delta(t)}{dt^2} < 0$	$w_\phi > w_0,\ \alpha_\phi < 0$
F	At this point, movement stops because the area A_2 is equal to the area A_1 and the machine goes back to a new stable place at point o	
o	$p_e = p_m,\ p_A = 0,\ \frac{d\delta(t)}{dt} = 0,\ \frac{d^2\delta(t)}{dt^2} = 0$	$w_\phi = w_0,\ \alpha_\phi = 0$
c	$p_e < p_m,\ p_A > 0,\ \frac{d\delta(t)}{dt} = 0,\ \frac{d^2\delta(t)}{dt^2} > 0$	$w_\phi = w_0,\ \alpha_\phi > 0$
b	$p_e < p_m,\ p_A > 0,\ \frac{d\delta(t)}{dt} < 0,\ \frac{d^2\delta(t)}{dt^2} > 0$	$w_\phi < w_0, \alpha_\phi > 0$
o	$p_e = p_m,\ p_A = 0,\ \frac{d\delta(t)}{dt} = 0,\ \frac{d^2\delta(t)}{dt^2} = 0$	$w_\phi = w_0,\ \alpha_\phi = 0$

Table 2
The details of the relationships between the position of the operating point on the p–δ curve and the w_ϕ–α_ϕ plane in the case of unstable swing.

Operating point	The generator angle changes in o-d-e-f-g points	
	Angular velocity and acceleration of δ	Angular velocity and acceleration of $\phi(t)$
o	$p_e = p_m,\ p_A = 0,\ \frac{d\delta(t)}{dt} = 0,\ \frac{d^2\delta(t)}{dt^2} = 0$	$w_\phi = w_0,\ \alpha_\phi = 0$
d	$p_e > p_m,\ p_A < 0,\ \frac{d\delta(t)}{dt} = 0,\ \frac{d^2\delta(t)}{dt^2} < 0$	$w_\phi = w_0,\ \alpha_\phi < 0$
e	$p_e > p_m,\ p_A < 0,\ \frac{d\delta(t)}{dt} > 0,\ \frac{d^2\delta(t)}{dt^2} < 0$	$w_\phi > w_0,\ \alpha_\phi < 0$
f	At this point, the area A_1 is greater than the area A_2 and the generator goes to an out-of-step condition	
g	$p_e < p_m, p_A > 0, \frac{d\delta(t)}{dt} > 0,\ \frac{d^2\delta(t)}{dt^2} > 0$	$w_\phi > w_0,\ \alpha_\phi > 0$

exciter with saturation limits are modeled in this research. Saturation function imposes lower and upper bounds on a signal. When the input signal is between the lower and upper limit values, it passes through unchanged; otherwise, the signal is clipped to the upper or lower bound. Therefore, once the generator violates its lower and upper (saturation) limits it cannot generate extra reactive power and will no longer contribute in sustaining the voltage in the network. Impact of saturation on the performance of the proposed method for a typical synchronous generator during the out-of-step situation is presented in Fig. 6.

Fig. 6(a) illustrates the field voltage of generator. As it is expected, the field voltage practically remains at its upper and lower bounds during the out-of-step condition. Besides, Fig. 6(b) shows the rotor angle and air-gap flux of a typical synchronous generator during unstable power swing with the absence and presence of the saturation phenomenon. In these figures, it can be clearly seen that saturation due to exciter operation has no important effect on the performance of the proposed relay.

2.4.2. *Saturation due to the load types of the power network*

The three load types in the power system are resistive, inductive, and capacitive. Magnetic saturation of a synchronous generator in the power system may occur due to the capacitive load of the power network. However, most of the loads are of inductive nature (3-ph

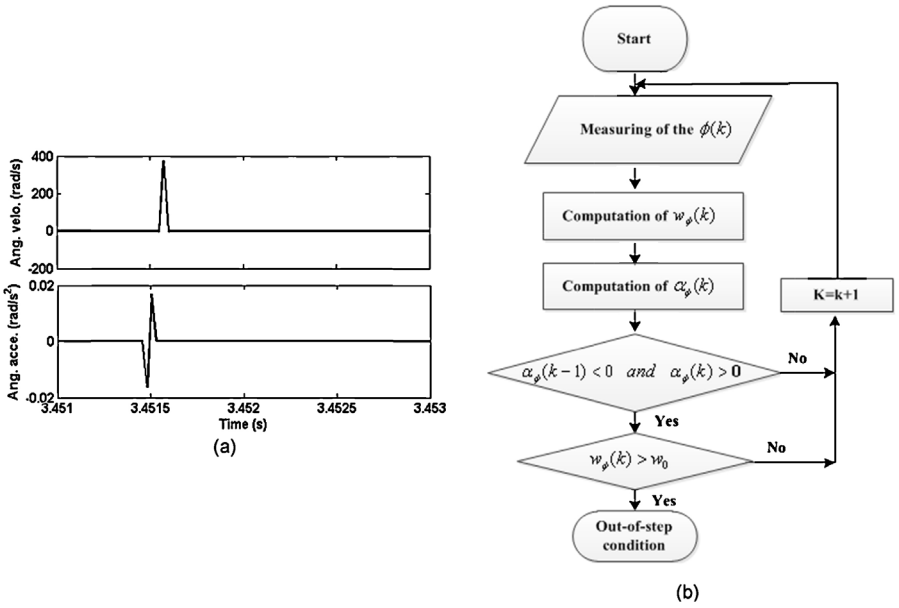

Fig. 5. Out-of-step condition: (a) a zoom in on the typical behavior of the angular velocity and acceleration data measured from the magnetic flux of a generator following out-of-step condition; (b) flowchart for the proposed method.

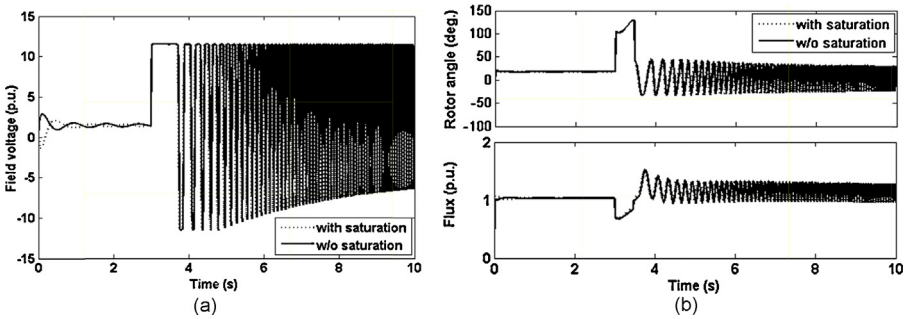

Fig. 6. Impact of saturation on the performance of the proposed method for a typical synchronous generator during the out-of-step condition: (a) field voltage of generator and (b) rotor angle and air-gap flux of generator.

induction motors, lighting, air conditioner, etc.). These loads are a major part of the system load [21]. Since the loads are inductive in nature, the probability of generator saturation occurrence due to the load types is very low. More details concerning this concept are presented in [17]. Furthermore, as stated earlier, in out-of-step condition the power system loses synchronisms due to a disturbance such as short-circuit faults, line switching, generator tripping, load shedding, etc. If this disturbance is a short-circuit fault, the magnetic saturation will not occur. In fact, the short-circuit characteristic is for all practical purposes linear because in this short-circuit condition the flux levels in the generator are below the level of iron saturation.

3. Performances of flux-based relay for out-of-step detection

In this section, the performance of flux-based out-of-step relay has been tested at different initial generator angles and loading conditions on two models of power system.

3.1. Case studies

In order to verify the advantages of the proposed solution, two power systems are considered to evaluate the performance of the proposed method on an SMIB and a TMIB configuration (Fig. 7(a) and (b)). In these configurations, generator 1 is equipped with a flux-based relay. The main parameters of the two power systems are given in Appendix [4,22–24]. It is worth mentioning that to analyze out-of-step condition, accurate dynamic modeling of synchronous machines, governors, power system stabilizers (PSSs) and exciters are of great importance. In these two power systems, all of synchronous generators contain PSS, excitation system and hydraulic turbine. These systems are illustrated in Fig. 7(c). In order to model the PSS, the governor and excitation systems, the models presented in [22–24] have been used. On the other hand, according to the machine capability curve, the operating loading points in per units used for generator 1 are presented in Table 3 and different simulation studies with initial generator angle 20° and 30° were conducted. These simulation strategies were performed considering 10 lagging and 10 leading power factor operation conditions with the effect of governor, AVR and PSS.

In the following, due to space limitations, most critical conditions will be presented and discussed to evaluate the performance of flux-based out-of-step relay. The results for these simulations are summarized in Tables 4 and 5.

These results show that under AVR operation, magnetic flux is approximately independent of load level. Using the proposed method, it can be clearly seen that out-of-step detection time changes slightly with different loading conditions. As stated

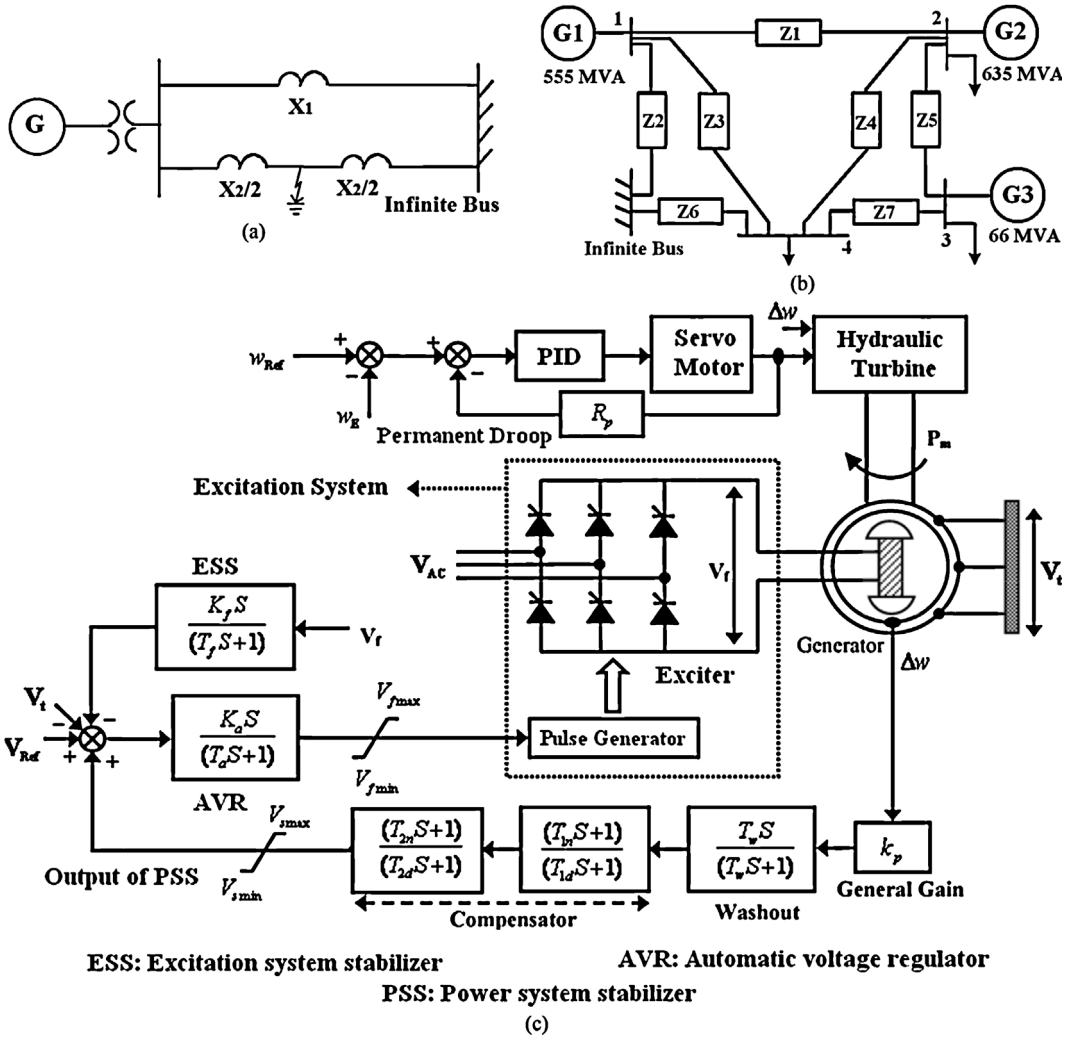

Fig. 7. The system studied: (a) SMIB system [4]; (b) TMIB system [4]; (c) block diagram of the excitation, PSS and governor system [22–24].

Table 3
Loading of generator.

$S=(P+jQ)$ p.u.							
L1	$0.1+j0.5$	L6	$0.5+j0.4$	L11	$0.9-j0.2$	L16	$0.5-j0.6$
L2	$0.1+j0.2$	L7	$0.7+j0.2$	L12	$0.7-j0.2$	L17	$0.3-j0.6$
L3	$0.3+j0.2$	L8	$0.7+j0.4$	L13	$0.7-j0.5$	L18	$0.3-j0.4$
L4	$0.3+j0.5$	L9	$0.9+j0.3$	L14	$0.5-j0.2$	L19	$0.3-j0.2$
L5	$0.5+j0.2$	L10	$0.9+j0.1$	L15	$0.5-j0.4$	L20	$0.1-j0.6$

earlier, AVR controls the output voltage and the magnetic flux of the machine, proportional to load level by controlling its excitation current. Therefore the load level would not cause any large fluctuation in the magnetic flux and the output voltage of the machine connected to light load and heavy load.

Fig. 8(a) illustrates the variation of rotor angle and magnetic flux of a 555 MVA synchronous generator at loading $L=0.9+j0.3$ p.u. during normal operation. According to Fig. 8(a), it can be clearly seen that for this condition, both flux and rotor angle are constant and have no oscillations. On the other hand, as stated earlier, magnetic flux is selected as the main criterion for out-of-step detection.

Therefore, to show the similarity in characteristics, Fig. 8(b) illustrates the characteristic of the magnetic flux of three different size generators at loading $L=0.9+j0.3$ per unit on the generator basis on SMIB configuration for stable power swing. It can be clearly seen that the magnetic flux variation has a unique behavior in all cases and its performance is not affected by the machine size.

Fig. 8(c) shows the rotor angle and magnetic flux of the 555 MVA synchronous generator on SMIB configuration with both absence and presence of the PSS in a stable power swing condition. For creating the stable swing condition, a three-phase fault is applied three seconds after the start of the simulation time at the middle of transmission line for the duration of 12 cycles (0.2 s) when the initial angle of the generator is set to 20°. It can be clearly seen that, the presence of the PSS causes better dampen stable power swings. In other words, PSS reduces the probability that a stable power swing will enter the impedance zone of a distance relay. This is due to the fact that PSS provides enough positive synchronizing and damping torques acting on the rotor of the generator. The angular velocity and acceleration of the magnetic flux of the generator are shown in Fig. 8(d). The angular velocity w_ϕ is less than w_0 when the sign of the angular acceleration α_ϕ changes from negative to positive, then, the out-of-step situation cannot be satisfied by the proposed method. In other words, the proposed method detects the swing as stable.

Fig. 9(a) shows the rotor angle and magnetic flux of the 555 MVA synchronous generator on SMIB configuration for unstable power swing during case 1 with the absence and presence of the PSS. In this case, the initial angle of the generator is set to 20° and a three-phase fault is applied at the middle of transmission line with a fault duration time of 0.3 s. In this condition, the stability is lost in both cases of presence and absence of the PSS, i.e. the out-of-step condition has happened. As stated in [1], and according to this figure, it

Table 4
Performance of flux-based out-of-step on an SMIB power system.

Case	Initial angle (°)	Type of loading (p.u.)	Fault duration time (s)	Detection time (s)
1	20	L9 = 0.9 + *j*0.3, Heavy, Lagging	0.1	Stable
			0.2	Stable
			0.25	0.451
			0.3	0.409
2	30	L9 = 0.9 + *j*0.3, Heavy, Lagging	0.1	Stable
			0.2	Stable
			0.25	0.4523
			0.3	0.43
3	20	L2 = 0.1 + *j*0.2, Light, Lagging	0.1	Stable
			0.2	Stable
			0.25	0.452
			0.3	0.62
4	30	L2 = 0.1 + *j*0.2, Light, Lagging	0.1	Stable
			0.2	Stable
			0.25	0.452
			0.3	0.661
5	20	L13 = 0.7 − *j*0.5, Heavy, Leading	0.1	Stable
			0.2	Stable
			0.25	0.435
			0.3	0.45
6	30	L13 = 0.7 − *j*0.5, Heavy, Leading	0.1	Stable
			0.2	Stable
			0.25	0.452
			0.3	0.481
7	20	L19 = 0.3 − *j* 0.2, Light, Leading	0.1	Stable
			0.2	Stable
			0.25	0.4178
			0.3	0.47
8	30	L19 = 0.3 − *j* 0.2, Light, Leading	0.1	Stable
			0.2	Stable
			0.25	0.42
			0.3	0.482

Table 5
Performance of flux-based out-of-step on a TMIB power system.

Case	Initial angle (°)	Type of loading (p.u.)	Fault duration time (s)	Detection time (s)
9	20	L9 = 0.9 + *j*0.3, Heavy, Lagging	0.1	Stable
			0.2	Stable
			0.25	0.403
			0.3	0.395
10	30	L9 = 0.9 + *j*0.3, Heavy, Lagging	0.1	Stable
			0.2	Stable
			0.25	0.401
			0.3	0.394
11	20	L2 = 0.1 + *j*0.2, Light, Lagging	0.1	Stable
			0.2	Stable
			0.25	0.451
			0.3	0.595
12	30	L2 = 0.1 + *j*0.2, Light, Lagging	0.1	Stable
			0.2	Stable
			0.25	0.455
			0.3	0.602
13	20	L13 = 0.7 − *j*0.5, Heavy, Leading	0.1	Stable
			0.2	Stable
			0.25	0.472
			0.3	0.53
14	30	L13 = 0.7 − *j*0.5, Heavy, Leading	0.1	Stable
			0.2	Stable
			0.25	0.472
			0.3	0.53
15	20	L19 = 0.3 − *j*0.2, Light, Leading	0.1	Stable
			0.2	Stable
			0.25	0.452
			0.3	0.501
16	30	L19 = 0.3 − *j* 0.2, Light, Leading	0.1	Stable
			0.2	Stable
			0.25	0.462
			0.3	0.506

can be clearly seen that during unstable power swing the presence of the PSS has no important effect on the dampen power swings seen by the generator. Generally speaking, PSS's are not effective in averting first swing instability. This is due to the fact that a significant reduction in the damping torques occurs that eventually causes loss of synchronism.

In this case, because the angular velocity w_ϕ is greater than w_0 when the angular acceleration α_ϕ changes from negative to positive, the out-of-step situation can be satisfied by the proposed method. For this unstable power swing, the out-of-step detection by the proposed method is satisfied 0.451 s (3.451 − 3) after the inception of the three-phase fault. It is worth mentioning that rapid detection of the out-of-step condition is desirable. The out-of-step condition must be rapidly distinguished before loss of synchronism, and to avoid generator damage, the generator must be isolated from the system. As a point of interest, according to this figure, it can be clearly seen that the proposed method detects the swing as unstable before loss of synchronism.

On the other hand, Fig. 9(b) shows the effect of stable power swing condition on the 555 MVA synchronous generator rotor angle and air-gap flux during case 9 with or without using PSS on the multi-machine configuration. In this case, the out-of-step condition cannot be satisfied by the proposed method. In other words, the proposed method detects the swing as stable on the multi-machine configuration.

Fig. 9(c) illustrates the rotor angle and air-gap flux of the 555 MVA synchronous generator on TMIB configuration for unstable power swing during case 9 with the absence and presence of the PSS. The initial angle of the generator is set to 20° and a three-phase fault is applied at the generator 1 terminal (Bus 1) with a fault duration time of 0.3 s. In this condition, the stability is lost, i.e. the out-of-step condition has happened. In this unstable power swing, the out-of-step detection by the proposed

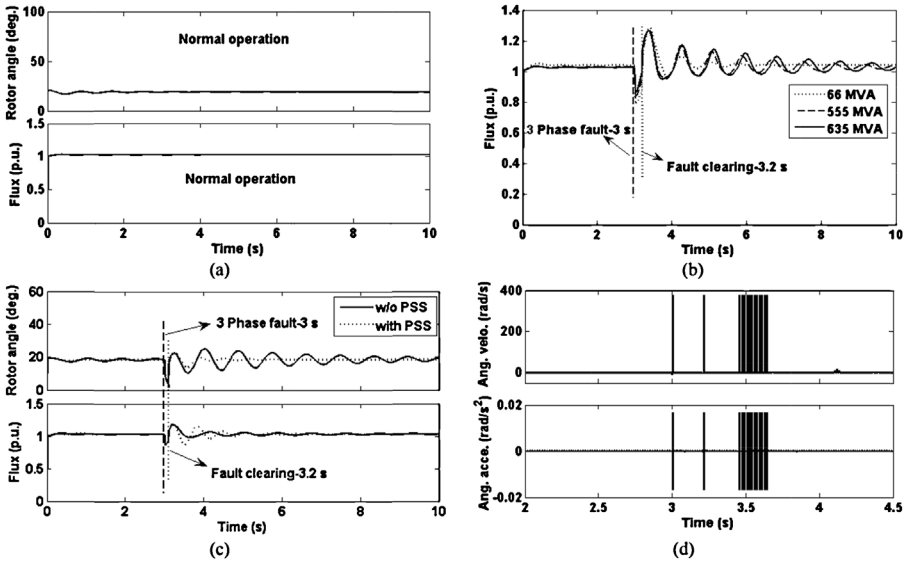

Fig. 8. Impact of a normal and stable power swing (SPS) conditions on the synchronous generator during case 1 on SMIB configuration. The initial angle of the generator is set to 20°. (a) Rotor angle and air-gap flux of a 555 MVA generator for normal operation. (b) Behavior of the air-gap flux of three size generators for SPS operation. (c) Rotor angle and air-gap flux of a 555 MVA generator for SPS operation with the absence and presence of the PSS. (d) Angular velocity and acceleration of the magnetic flux of a 555 MVA generator for SPS operation.

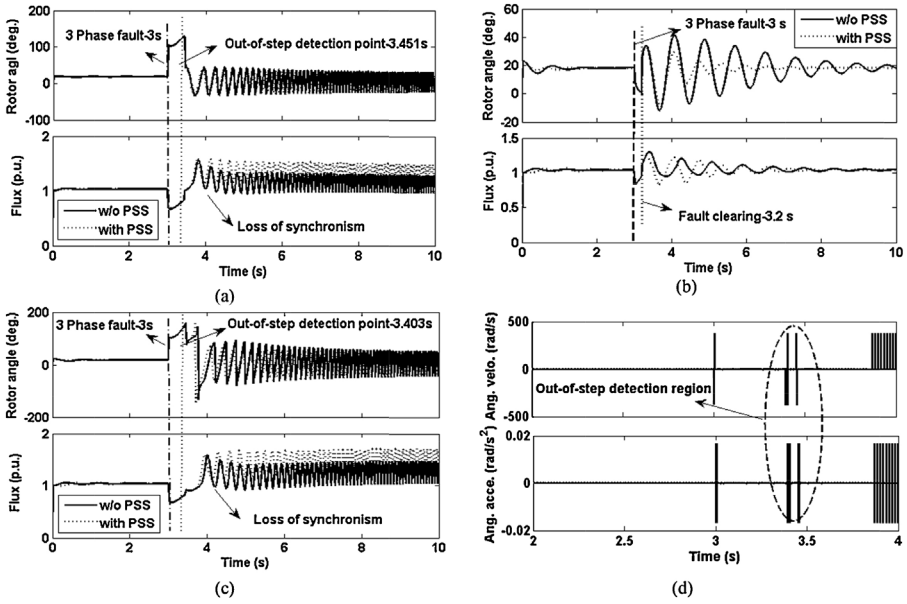

Fig. 9. Impact of a SPS and unstable power swing on a 555 MVA synchronous generator during cases 1and 9 on SMIB and TMIB configuration. The initial angle of the generator is set to 20° and fault cleared after 0.2 s and 0.3 s for SPS and unstable power swing conditions, respectively. (a) Rotor angle and air-gap flux of the generator during case1 for unstable power swing condition with or without using PSS. (b) Rotor angle and air-gap flux of the generator during case 9 for SPS condition with the absence and presence of the PSS. (c) Rotor angle and air-gap flux of the generator during case 9 for unstable power swing condition with or without using PSS. (d) Angular velocity and acceleration of the magnetic flux of the generator during case 9 for unstable power swing condition.

method is satisfied 0.403 s (3.403 − 3) after the inception of the three-phase fault. According to Fig. 9(c), it can be clearly seen that the magnetic flux of generator 1 on the multi-machine power system has a similar behavior to magnetic flux of the generator on SMIB power system (Fig. 9(a)). However, the multi-machine power system slightly changes the detection time compared to the SMIB power system. For this condition, the angular velocity and acceleration of the magnetic flux of the generator are illustrated in Fig. 9(d). By comparing the effect of PSS on the rotor oscillations in the SMIB and TMIB systems, it is evident that generally the results of these cases are similar, i.e. the presence of the PSS causes better dampen stable power swings while during unstable power swing the PSS has no important effect on the dampen power swings.

The simulation studies illustrate that the proposed method is not only effective on an SMIB power network, but it is equally effective on a multi-machine power network. In the other words, the results on a TMIB power network show that the application of the proposed technique is straightforward, even for a multi-machine power system and can be directly applied to an interconnected power network without any need to cumbersome network reduction methods as well.

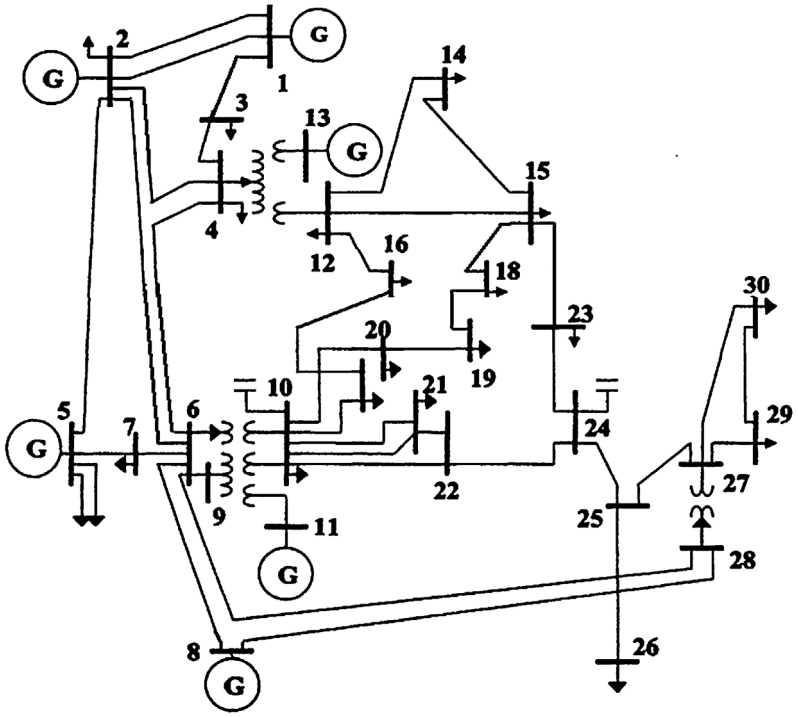

Fig. 10. IEEE 30 bus power system [25].

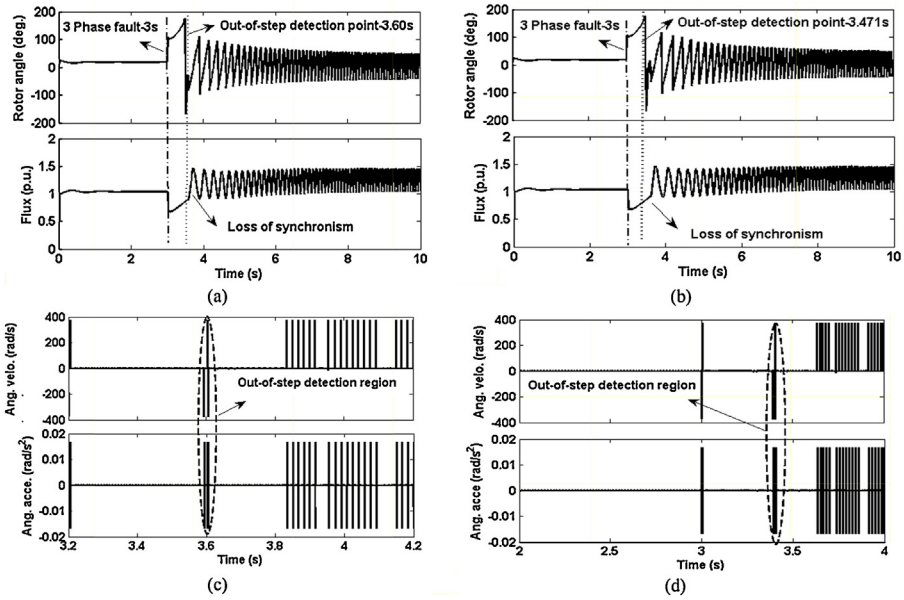

Fig. 11. Impact of unstable power swing on the synchronous generators in the IEEE 30 bus power system. The initial angle of the generator is set to 20° and fault cleared after 0.3 s for this condition. (a) Rotor angle and air-gap flux of generator on bus 1. (b) Rotor angle and air-gap flux of generator on bus 8. (c) Angular velocity and acceleration of the magnetic flux of generator on bus 1. (d) Angular velocity and acceleration of the magnetic flux of generator on bus 8.

4. Practical application of the proposed method

In order to show a practical application, the efficiency of the proposed algorithm has been tested on an IEEE 30-bus power system as shown in Fig. 10. The IEEE 30-bus test case represents a simple approximation of the American Electric Power system. The parameters of this power system are taken from Ref. [25] and it is simulated and implemented in "Matlab/Simulink". In this power system, generators on bus 1 and 8 are equipped with a flux-based relay. Several unstable test scenarios are created and the proposed method is found to perform well in all cases. The results on this multi-machine power network also show that the proposed algorithm is effective for a straightforward application to multi-machine systems without any need for system reduction.

As representative examples of the many simulations carried out on the system are studied, Fig. 11(a) and (b) show the rotor angle and magnetic flux of the generator 1 and 8 on this multi-machine power network for unstable power swing condition, respectively.

Table 6
Detection time comparisons for different methods on an SMIB power system.

Method	Initial angle = 20°, L9 = 0.9 + *j*0.3 p.u., Heavy load, lagging	
	Fault duration = 0.25 s	Fault duration = 0.3 s
	Detection time (s)	
Concentric rectangle	0.618	0.524
Power-time domain	0.598	0.504
Flux-based	0.4523	0.43

Table 7
Detection time comparisons of flux-based method for different size of generators on an SMIB power system.

Generator (MVA)	Fault duration = 0.25 s, Initial angle = 20°	
	L9 = 0.9 + *j*0.3 p.u., Heavy load, lagging	L19 = 0.3 − *j*0.2 p.u., light load, leading
	Detection time (s)	
66	0.62	0.5372
555	0.4519	0.4178
635	0.4513	0.43

In these cases the initial angle of the generators is set to 20° and a three-phase fault is applied at the related terminals (bus 1 and 8) with a fault duration time of 0.3s to create the unstable power swing condition. In these test cases, machine 1 and 8 were loaded to 90% and 70% of their maximum capacities, respectively. In these cases, the stability is lost, i.e. the out-of-step condition has happened and the out-of-step detection by the proposed method is satisfied 0.6 s (3.6 − 3) and 0.471 s (3.471 − 3) after the beginning of the three-phase fault, respectively. In these figures, it can be clearly seen that, the magnetic flux of the generator 1 and 8 on the IEEE 30 bus power system have a similar behavior to magnetic flux of the previous power systems (Fig. 9(a) and (c)). For these conditions, the angular velocity and acceleration of the magnetic flux of the generators are illustrated in Fig. 11(c) and (d).

It is worth highlighting that as stated earlier, magnetic flux is a local variable in the machine and this criterion will change locally due to the fault occurrence, whereas stator current and voltage are global external variables that are affected by different causes. Therefore, the new flux-based protection technique is independent of the power system configuration.

5. Comparative analysis

In order to validate the proposed technique, a comparative analysis is made between the proposed method, the conventional out-of-step relay and a power-time domain out-of-step relay results, presented in [4] (one of the latest article published in this field). Therefore, the power network parameters given in [4] have been used. The conventional relay used in this study is a concentric rectangle scheme as recommended by [1] in practice. The out-of-step detection times, using the flux-based method, concentric rectangle scheme and power-time domain technique is compared for the two conditions in case 2. In case 2 with a fault duration time of 0.25 s, as reported in [4] and according to simulation in this study, the concentric rectangular technique sends a trip signal in 0.618 s, power-time domain method in 0.598 s, and the flux-based method (proposed scheme) sends a trip signal in 0.4523 s from the inception of fault during the out-of-step condition. In case 2 with a fault duration time of 0.3 s, as reported in [4] and according to simulation in this study, the concentric rectangular method took 0.524 s, power-time domain method took 0.504 s, whereas the flux-based method (proposed scheme) took 0.43 s to make the required decision. Thus, in these conditions on an SMIB system, the proposed method operates in shorter time than other methods.

In other words, the flux-based method is fast and effective for detection of the out-of-step condition. The results of these comparisons are summarized in Table 6. Furthermore, to show the similarity in characteristics, Table 7 illustrates the detection time by the proposed method for different size machines connected to light load and heavy load on an SMIB power system. It is worth mentioning that, the out-of-step detection times using the flux-based method changes slightly with different loading and the generator size which has no important effect on the sensitivity of the proposed method.

6. Conclusion

The magnetic flux analysis technique has been used successfully for diagnosis of the internal faults and loss of excitation protection in synchronous generators by the author. In a continuation of the previous works, this paper proposed a new out-of-step protection method based on the analysis of the magnetic flux of the generator available at a local bus. The satisfactory operation of the proposed method has been verified via simulation studies on an SMIB and a TMIB power network. The results obtained from extensive case studies illustrate that the new flux-based relay has some advantages over existing methods. The first is that the proposed relay is able to detect out-of-step during various kinds of conditions. The second distinctive feature for the method intends to keep it independent of the machine size, parameters and the power system configuration. In addition, the proposed relay is independent from other generator protection relays without any coordination studies. Another point worth highlighting is that the proposed scheme also does not require any offline studies and solving any especial impedance calculation equations. This makes its application straightforward, even for a multi-machine power system and can be directly applied to an interconnected power network without any need to cumbersome network reduction methods.

Appendix A. Appendix

See Tables 8–10.

Table 8
SMIB parameters [4].

Generator rating = 555 MVA, 24 kV, Frequency = 60 Hz
X_d(p.u.) = 1.81, X'_d(p.u.) = 0.3, X''_d(p.u.) = 0.23, X_q(p.u.) = 1.76,
X'_q(p.u.) = 0.65, X''_q(p.u.) = 0.25, X_1(p.u.) = 0.15, $T'do(s)$ = 8,
$T''do(s)$ = 0.03, $T'qo(s)$ = 1, $T''qo(s)$ = 0.07, Rs(p.u.) = 0.003.
Inertia constant (H) = 3.5 s, Infinite bus voltage = 0.9 p.u.
Transformer = *j*0.15 p.u., TL-II = *j*0.5 p.u., TL-II = *j*0.93 p.u.

Table 9
TMIB parameters [4].

Generator-1 rating = 555 MVA, 24 kV, H = 3.5 s
Generator-2 rating = 635 MVA, 24 kV, H = 5.4 s
Generator-3 rating = 66 MVA, 24 kV, H = 4.29 s
$Z1$ = 0.048 + *j*0.48 ohm, $Z2$ = 0.00576 + *j*0.573 ohm
$Z3$ = 0.0288 + *j*0.288 ohm, $Z4$ = 0.0576 + *j*0.576 ohm,
$Z5$ = 0.0142 + *j*0.142 ohm, $Z6$ = 0.0192 + j0.192 ohm,
$Z7$ = *j*0.0957 ohm

Table 10
Parameters of the used PSS, AVR and hydraulic turbine combined to a PID governor system [22–24].

PSS		AVR		Hydraulic turbine and PID	
Parameters	Value	Parameters	Value	Parameters	Value
Gain	k_p(p.u.) = 30	Low-pass filter	$T_r(s) = 20e-3$	Servo-motor	k_a(p.u.) = 3.33, $T_a(s) = 0.07$
Wash-out	$T_w(s) = 10$	Regulator	k_a(p.u.) = 300, $T_a(s) = 0.001$	Droop	R_p(p.u.) = 0.05
1st Lead-lag	$T_{1n}(s) = 50e-3$, $T_{1d}(s) = 20e-3$	Damping filter	k_f(p.u.) = 0.001, $T_f(s) = 0.1$	Regulator	$k_p = 1.163$, $k_i = 0.105$, $k_d = 0$, $T_d(s) = 0.01$
2nd Lead-lag	$T_{2n}(s) = 3$, $T_{2d}(s) = 5.4$	Exciter	k_e(p.u.) = 1, $T_e(s) = 0$	Hydraulic turbine	$\beta = 0$, $T_w(s) = 2.67$
Output limits	$V_{s\max}$(p.u.) = 0.15, $V_{s\min}$(p.u.) = −0.15	Output limits	$V_{f\max}$(p.u.) = 11.5, $V_{f\min}$(p.u.) = −11.5	Gate opening limits	$g_{\min}$(p.u.) = 0.01, $V_{g\min}$(p.u./s) = −0.1 $g_{\max}$(p.u.) = 0.975, $V_{g\max}$(p.u./s) = 0.1

References

[1] IEEE Power System Relaying Committee Working Group D6, Power Swing and Out-of-step Considerations on Transmission Lines, 2005, June.
[2] E. Pajuelo, R. Gokaraju, M.S. Sachdev, Identification of generator loss-of-excitation from power-swing conditions using a fast pattern classification method, IET Gener. Transm. Distrib. 7 (1) (2013) 24–36.
[3] K.H. So, J.Y. Heo, R.K. Aggarwal, K.B. Song, Out-of-step detection algorithm using frequency deviation of voltage, IET Gener. Transm. Distrib. 1 (1) (2007) 119–126.
[4] S. Paudyal, G. Ramakrishna, M.S. Sachdev, Application of equal area criterion conditions in the time domain for out-of-step protection, IEEE Trans. Power Deliv. 25 (2) (2010) 600–609.
[5] N. Chothani, B. Bhalja, U. Parikh, New support vector machine-based digital relaying scheme for discrimination between power swing and fault, IET Gener. Transm. Distrib. 8 (1) (2014) 17–25.
[6] B. Shrestha, G. Ramakrishna, M.S. Sachdev, Out-of-step protection using state-plane trajectories analysis, IEEE Trans. Power Deliv. 28 (2) (2013) 1083–1093.
[7] A.Y. Abd-Elaziz, M.R. Irving, A.M. El-Arabaty, M.M. Mansour, Out-of-step prediction based on artificial neural networks, Electr. Power Syst. Res. 34 (1995) 135–142.
[8] H.E.A. Talaat, Predictive out-of-step relaying using fuzzy rule-based classification, Electr. Power Syst. Res. 48 (1999) 143–149.
[9] Y. Morioka, et al., System separation equipment to minimize power system instability using generator's angular-velocity measurements, IEEE Trans. Power Deliv. 8 (3) (1993) 941–947.
[10] H. Henao, C. Demian, G.-A. Capolino, A frequency-domain detection of stator winding faults in induction machines using an external flux sensor, IEEE Trans. Ind. Appl. 39 (5) (2003) 1272–1279.
[11] V.P. Bui, O. Chadebec, L.-L. Rouve, J.-L. Coulomb, Noninvasive fault monitoring of electrical machines by solving the steady-state magnetic inverse problem, IEEE Trans. Magn. 44 (6) (2008) 1050–1053.
[12] H. Yaghobi, H. Rajabi Mashhadi, K. Ansari, Artificial neural network approach for locating internal faults in salient-pole synchronous generator, Expert Syst. Appl. 38 (2011) 13328–13341.
[13] H. Yaghobi, K. Ansari, H. Rajabi Mashhadi, Stator turn-to-turn fault detection of synchronous generator using total harmonic distortion analyzing of magnetic flux linkage, Iran. J. Sci. Technol. Trans. Electr. Eng. (IJSTE) 37 (E2) (2013) 161–182.
[14] H. Yaghobi, K. Ansari, H. Rajabi Mashhadi, Analysis of magnetic flux linkage distribution in salient-pole synchronous generator with different kinds of inter-turn winding faults linkage, Iran. J. Electr. Electron. Eng. (IJEEE) 7 (4) (2011) 260–272.
[15] H. Yaghobi, Impact of static synchronous compensator on flux-based synchronous generator loss of excitation protection, IET Gener. Transm. Distrib. 9 (9) (2015) 874–883.
[16] H. Yaghobi, H. Mortazavi, A novel method to prevent incorrect operation of synchronous generator loss of excitation relay during and after different external faults, Int. Trans. Electr. Energy Syst. (ETEP) 25 (9) (2015) 1717–1735.
[17] H. Yaghobi, H. Mortazavi, K. Ansari, et al., Study on application of flux linkage of synchronous generator for loss of excitation detection, Int. Trans. Electr. Energy Syst. (ETEP) 23 (6) (2013) 802–817.
[18] A.E. Fitzgerald, C. Kingsley, S.D. Umans, Electric Machinery, 6th ed., Mc Graw-Hill, New York, 2003.
[19] G. Klempner, I. Kerszenbaum, Operation and Maintenance of Large Turbo-generators, John Wiley & Sons, New Jersey, 2004.
[20] P.J. Tavner, B.G. Gaydon, B.A. Ward, Monitoring generators and large motors, Proc. IEE 133 (3 (Pt. B)) (1986) 169–180.
[21] G. Shrinivasan, Power System Analysis, 2nd ed., Technical Publications, Pune, India, 2009.
[22] IEEE Std. 421.5, Recommended Practice for Excitation System models for Power System Stability Studies, 1992.
[23] IEEE working group on prime mover and energy supply models for system dynamic performance studies, Hydraulic turbine and turbine control models for dynamic studies, IEEE Trans. Power Syst. 7 (1) (1992) 167–179.
[24] A. Ghorbani, B. Mozafari, S. Soleymani, A.M. Ranjbar, Operation of synchronous generator LOE protection in the presence of shunt-FACTS, Electr. Power Syst. Res 119 (2015) 178–186.
[25] C. Mishra, S.P. Singh, J. Rokadia, Optimal power flow in the presence of wind power using modified cuckoo search, IET Gener. Transm. Distrib. 9 (7) (2015) 615–626.